

## PRELIMINARY STUDY FOR COVID-19 DRUG DISCOVERY OF 30 PHYTOCHEMICAL COMPOUNDS FROM *TETRAGONULA SP.* PROPOLIS AS PAK1 INHIBITOR THROUGH MOLECULAR DOCKING

SAFIRA CANDRA ASI<sup>H1</sup>, MUHAMAD SAHLAN<sup>1,2</sup>, MOHAMMAD NASIKIN<sup>1\*</sup>

<sup>1</sup>Department of Chemical Engineering, Faculty of Engineering, Universitas Indonesia, Depok, 16424, Indonesia, <sup>2</sup>Research Center for Biomedical Engineering, Universitas Indonesia, Depok, 16424, Indonesia  
\*Email: mnasikin@che.ui.ac.id

Received: 20 Dec 2021, Revised and Accepted: 24 Mar 2022

### ABSTRACT

**Objective:** This study aims to evaluate 30 phytochemical compounds from *Tetragonula sp.* propolis as a PAK1 inhibitor using molecular docking.

**Methods:** Thirty propolis compounds were initially confirmed before docking to comply with Lipinski rules. This simulation was performed against PAK1 using AutodockVina, while interaction profile visualization was conducted between the ligand and receptor through Ligplot+ and PyMol.

**Results:** Based on the docking score, inhibition constants, and interaction profile analyses, glyurallin B, glyasperin A, and broussonflavonol F were found to be the most potent compounds used as PAK1 inhibitors. According to several literature studies, the propolis compounds were synergistic, leading to adequate collective utilization.

**Conclusion:** These results implicated the potentials of *Tetragonula sp.* propolis as a therapeutic agent against COVID-19; however, further studies are still needed.

**Keywords:** PAK1, Propolis, *Tetragonula Sp.*, COVID

© 2022 The Authors. Published by Innovare Academic Sciences Pvt Ltd. This is an open access article under the CC BY license (<https://creativecommons.org/licenses/by/4.0/>)  
DOI: <https://dx.doi.org/10.22159/ijap.2022.v14s3.25> Journal homepage: <https://innovareacademics.in/journals/index.php/ijap>

### INTRODUCTION

Several individuals reportedly suffered from pneumonia in December 2019 in Wuhan, Hubei province, China. This ailment showed similar symptoms of SARS (severe acute respiratory syndrome), although it was subsequently identified as a coronavirus (COVID-19) by the World Health Organization (WHO), indicating the discovery of SARS-CoV-2 (severe acute respiratory syndrome-coronavirus-2) as the causative agent. Also, the direct human-to-human transmission was confirmed, leading to extensive and faster virus distribution. By December 1st, 2021, global statistics had regrettably recorded approximately 217 million positive confirmed cases, with 4.5 million leading to death [1]. Based on this condition, only two drugs have been presently approved by the FDA to treat COVID-19. Therefore, the exploration of new medicines and vaccines is conducted to present diverse opportunities. Furthermore, based on this pandemic, there is a need to adopt virtual screening procedures due to high pressure to develop fast and reliable drugs through molecular docking. This computational method simulates the ligand-receptor complex's most optimal position [2]. This is performed by using the minimum scoring function or free energy of the entire system [3, 4]. The technique also served as a confirmed medium to comprehend the interaction of compounds and new drug discovery since its development in the 1970s [5].

Based on this study, the receptor protein used is the PAK1 (p21-activated kinase 1) enzyme, whose inactivation/inhibition suppresses the LLC2-dependent fibrosis induced by a coronavirus [6]. This is because LLC2 expression is dependent on the CK2/RAS-PAK1-RAF-AP1 signaling pathway induced by the ACE2 (angiotensin-converting enzyme 2) coronavirus receptor [7, 8]. These observations demonstrate the contribution of PAK1 to the pathogenesis of the coronavirus, which is a viable target protein for the search of COVID-19 drugs through enzymatic inhibitors. Although several studies have potentially described propolis as therapeutic for COVID-19 treatment due to its pharmacological characteristics [9-12], it is still found to vary in geographical composition. Previous investigations also confirmed the pharmacological characteristics of propolis, including antifungal, antioxidant, and anti-inflammatory properties [13]. Based on Miyata *et al.* (2019), a total of 30 compounds were identified from

*Tetragonula sp.* propolis [13], with LC-MS being evaluated using the molecular docking method to PAK1 (PDB ID: 5DEW). This indicated that the utilized evaluation parameters were docking score, inhibition constant, and interaction profile.

### MATERIALS AND METHODS

#### Main protein and ligand preparation

The main protein file (PDB ID: 5DEW) was extracted from the RCSB Data Bank (<http://www.rcsb.org>), where PAK-1 was in complex with inhibitor G-5555. Using the VMD software (the University of Illinois at Urbana-Champaign, USA), this complex was subsequently separated with visual molecular dynamics and saved in .pdb format before editing with notepad++ (Don Ho, USA). Furthermore, the polar hydrogen was added to the main protein through AutoDock 1.5.6 (The Scripps Research Institute, USA). Meanwhile, the 2D and 3D structures of the test compounds were developed using MarvinSketch software, which was also used to assess the Lipinski rules. The test compounds were also re-evaluated with the SwissADME web tool (<http://www.swissadme.ch/>) to ascertain the drug likeness and bioavailability. In addition, polar hydrogen was added to these compounds using the Auto-Dock 1.5.6 and saved in .pdb format (The Scripps Research Institute, USA).

#### Validation of the grid box area and coordinates for docking

To utilize the AutoDock Vina program for molecular docking, the grid box area and coordinates were required. These inputs were subsequently obtained from the redocking process between PAK-1 and G-5555, using AutoDock 1.5.6 and Vina (The Scripps Research Institute, USA), respectively. Moreover, the redocking coordinates had a 'centered on ligand' format on the grid box menu, with a 1 Å spacing. The docking area was specified as 25 Å x 25 Å x 25 Å. From the redocking process, it will be obtained ten docking poses with the binding affinity values. The coordinate from the pose, which has the lowest docking score, was used. By determining the root-mean-square deviation (RMSD), the coordinate was subsequently evaluated for similarities to the developed model using PyMOL (Schrödinger, Inc., USA). The validation process is considered successful if the RMSD value is less than 2.0 Å [14].

### Molecular docking

The molecular docking between 30 compounds was performed against PAK1 through the AutoDock Vina (The Scripps Research Institute, USA). These compounds are subsequently presented in table 1. Furthermore, the grid box dimensions and coordinates were obtained from the previous redocking step, as the genetic algorithm

parameters were set to default, where the population size was observed at 150. Furthermore, the maximum evaluation and generations were also set to medium and 27,000, respectively, with the top automatically-survived individuals at 1. Also, the rates of gene mutation and crossover were specified at 0.02 and 0.8, respectively. Subsequently, the remaining docking parameters were modified to default.

**Table 1: 30 Compound from *Tetragonula sp. propolis***

Name	Code	Chemical formula
L-(+)-Valinol	WR01	C <sub>5</sub> H <sub>13</sub> NO
1,2,2-Trimethyl-3-[[4-methylphenyl] carbamoyl] cyclopentane carboxylic acid	WR02	C <sub>17</sub> H <sub>23</sub> NO <sub>3</sub>
Linalyl anthranilate	WR03	C <sub>17</sub> H <sub>23</sub> NO <sub>2</sub>
Yucalexin B7	WR04	C <sub>20</sub> H <sub>28</sub> O <sub>2</sub>
Robustaol A	WR05	C <sub>25</sub> H <sub>30</sub> O <sub>9</sub>
1,5-Dimethyl-4-[[[(2-methyl-6-phenylthieno[2,3-d]pyrimidin-4-yl)hydrazinylidene]methyl]pyrrol E-2-carbonitrile	WR06	C <sub>21</sub> H <sub>18</sub> N <sub>6</sub> S
Kadsurin	WR07	C <sub>25</sub> H <sub>30</sub> O <sub>8</sub>
5-Hydroxymethyl tolterodine	WR08	C <sub>22</sub> H <sub>31</sub> NO <sub>2</sub>
Dulxanthone C	WR09	C <sub>25</sub> H <sub>28</sub> O <sub>6</sub>
9'-Carboxy-alpha-tocotrienol	WR10	C <sub>24</sub> H <sub>34</sub> O <sub>4</sub>
Enokipodin D	WR11	C <sub>15</sub> H <sub>18</sub> O <sub>4</sub>
Mollicellin H	WR12	C <sub>21</sub> H <sub>20</sub> O <sub>6</sub>
Glyurallin B	WR13	C <sub>25</sub> H <sub>26</sub> O <sub>6</sub>
[[8]-Paridyl acetate)	WR14	C <sub>21</sub> H <sub>32</sub> O <sub>4</sub>
Macarangin	WR15	C <sub>25</sub> H <sub>26</sub> O <sub>6</sub>
3,4-Bis(octyloxy)benzaldehyde	WR16	C <sub>21</sub> H <sub>38</sub> O <sub>3</sub>
Oleandrigenin	WR17	C <sub>25</sub> H <sub>36</sub> O <sub>6</sub>
Sulabiroin A	KM01	C <sub>22</sub> H <sub>22</sub> O <sub>7</sub>
Sulabiroin B	KM02	C <sub>23</sub> H <sub>26</sub> O <sub>7</sub>
2',3'-Dihydro-3'-hydroxypapuanic acid	KM03	C <sub>25</sub> H <sub>38</sub> O <sub>7</sub>
(-)-papuanic acid	KM04	C <sub>25</sub> H <sub>36</sub> O <sub>6</sub>
(-)-isocalolongic acid	KM05	C <sub>23</sub> H <sub>32</sub> O <sub>6</sub>
Isopapuanic acid	KM06	C <sub>25</sub> H <sub>36</sub> O <sub>6</sub>
Isocalopolyanic acid	KM07	C <sub>24</sub> H <sub>32</sub> O <sub>6</sub>
Glyasperin A	KM08	C <sub>25</sub> H <sub>26</sub> O <sub>7</sub>
Brousoflavonol F	KM09	C <sub>25</sub> H <sub>26</sub> O <sub>7</sub>
(2S)-5,7-Dihydroxy-4'-methoxy-8-prenylflavanone	KM10	C <sub>20</sub> H <sub>20</sub> O <sub>5</sub>
Isorhamnetin	KM11	C <sub>16</sub> H <sub>12</sub> O <sub>7</sub>
(1'S)-2-Trans,4-trans-abscisic acid	KM12	C <sub>15</sub> H <sub>20</sub> O <sub>4</sub>
(1'S)-2-Cis,4-trans-abscisic acid	KM13	C <sub>15</sub> H <sub>20</sub> O <sub>4</sub>

### Analysis and visualization

The best-predicted poses were obtained from the docking simulation and subsequently analyzed by PyMol (Schrödinger, Inc., New York, NY, USA). Also, the 2D ligand schematic representations and interacted residues within the receptor's binding site were developed using LigPlot+(European Bioinformatics Institute, United Kingdom).

### Analysis of the synergistic effect

The analysis of synergistic effect is based on a literature study by comparing several studies towards the existence of synergistic effect in propolis.

## RESULTS AND DISCUSSION

### Evaluation of the lipinski rules and swissADME parameters

The test compounds were initially evaluated using the Lipinski rule [15] to assess specific element parameters, including absorption, distribution, metabolism, and excretion. These factors were found to influence the pharmacokinetic properties in the human body [16]. Molecules were also considered to demonstrate suitable drug-likeness and bioavailability due to the achievement of 2 regulations from four existing rules [17]. Furthermore, each Lipinski parameter value was ascertained using the Marvin Sketch application.

**Table 2: Lipinski rule**

Parameter	Value	
Molecular weight (MW)	<500g/mol	Passing the criteria if it meets 2 of the 4 existing rules
LogP	<5	
Hydrogen donor	<5	
Hydrogen acceptor	≤10	

Based on this study, the Swiss ADME application provided a web-based alternative in evaluating the drug-likeness and bioavailability of test compounds [18]. This computed and predicted the physicochemical descriptors and ADME variables, such as the

pharmacokinetics profiles, drug-like nature, and medicinal chemistry friendliness of small molecules. Based on table 2, all compounds met the drug-likeness criteria evaluated by the Lipinski Rules and Swiss ADME.

Table 2: The Evaluation of drug likeness of a compound using lipinski rules and SwissADME webtool

Compound code <sup>1</sup>	Lipinski R05 parameter				Meet R05 criteria	Meet SwissADME <sup>2</sup>
	MW (g/mol)	LogP	H donor	H acceptor		
WR01	103.16	0	2	2	Yes	Yes
WR02	289.37	3	2	3	Yes	Yes
WR03	273.37	4.83	1	2	Yes	Yes
WR04	300.44	3.76	0	2	Yes	Yes
WR05	474.50	5.19	5	9	Yes	Yes
WR06	386.47	4.76	1	6	Yes	Yes
WR07	458.50	4.59	0	8	Yes	Yes
WR08	341.49	4.39	2	3	Yes	Yes
WR09	424.49	6.6	2	6	Yes	Yes
WR10	386.52	6.14	2	4	Yes	Yes
WR11	262.3	0.78	1	4	Yes	Yes
WR12	101	4.9	2	6	Yes	Yes
WR13	422.47	6.16	4	6	Yes	Yes
WR14	348.48	5.64	0	4	Yes	Yes
WR15	422.47	6.3	4	6	Yes	Yes
WR16	362.55	8.1	0	3	Yes	Yes
WR17	432.55	1.93	2	6	Yes	Yes
KM01	398.41	3.38	0	7	Yes	Yes
KM02	414.45	3.51	0	7	Yes	Yes
KM03	450.57	5.35	3	7	Yes	Yes
KM04	432.55	6.73	2	6	Yes	Yes
KM05	404.50	5.64	2	6	Yes	Yes
KM06	432.55	6.73	2	6	Yes	Yes
KM07	416.51	5.3147	2	6	Yes	Yes
KM08	422.47	5.75	4	6	Yes	Yes
KM09	422.47	6.37	4	6	Yes	Yes
KM10	354.40	4.64	2	5	Yes	Yes
KM11	316.26	1.87	4	7	Yes	Yes
KM12	264.32	1.61	2	4	Yes	Yes
KM13	264.32	1.61	2	4	Yes	Yes

<sup>1</sup>The information on the compound's name and chemical formula for each code is contained in the supplementary data (Supplementary material Appendix 1, fig. A1), <sup>2</sup>The evaluation process involves inserting SMILES data of each phytochemical compound into the SwissADME web tool: <http://www.swissadme.ch/> to produce absorption, distribution, metabolism, and excretion results (ADME).

### Validation of grid box area and coordinates for docking

The RMSD is used to validate the grid box area and coordinates for docking due to being closely related to the position between 2 atoms (protein and ligand). Also, it is defined as the average distance between the atoms of the superimposed protein molecules. In this

study, the RMSD was between the best-docked pose from the PAK1 redocking process against the ligand G-5555 and RCSB developed model (PDB ID: 5DEW). According to table 3, the RMSD met the requirements to be  $\leq 2$ . Therefore, the grid box area and coordinates information focused on the docking process between PAK-1 and the 30 test compounds.

Table 3: Grid box area, docking coordinates and its RMSD value

Grid box area	Coordinates	RMSD
x=25 Å	x=19.295	1.253
y=25 Å	y=-13.282	
z=25 Å	z=11.782	

### Docking score and inhibition constant

Free binding energy or docking score ( $\Delta G$ ) served as a parameter for evaluating the affinity of a ligand interaction (test compound) with its receptor (target protein) [19]. This is calculated using the following equation 1,

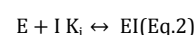
$$\Delta G_{\text{binding}} = \Delta H - T\Delta S \text{ (Eq. 1)}$$

Where  $\Delta H$  and  $T\Delta S$  were the enthalpy and entropy, respectively. In molecular docking, a negative  $\Delta G$  value was often the desired result. Moreover, increasing the negativity of  $\Delta G$  generated extensive affinity and more vigorous interaction between the ligand and the receptor. The negativity of  $\Delta G$  was triggered by the binding process, where the enthalpy decreased due to the intermolecular interactions and bond formation. However, the entropy increased based on losing the degrees of freedom, leading to a negative  $\Delta G$ .

According to fig. 1, the docking score for each compound towards PAK1 was observed, indicating that the interaction of G5555 towards

PAK1 served as the positive control. The results showed that the score ranged between -3.8 to -8.9 kcal/mol, compared to the control positive of -9.6 kcal/mol. Although none of the test compounds' interactions had a docking score less than the original ligand, negative values were still observed. This indicated that all test compounds bonded with the protein. In addition, the top ten propolis compounds with the lowest docking score are presented in table 4.

The results showed that the  $\Delta G$  value was altered to obtain the inhibition constant ( $K_i$ ) or dissociation coefficient ( $K_d$ ) in the enzyme (E)-inhibitor (I) complex [20].



$$\Delta G_{\text{inhibition}} = RT \ln K_i \text{ (Eq.3)}$$

$$K_i = \exp\left(\frac{\Delta G}{RT}\right) \text{ (Eq.4)}$$

Where  $\Delta G$  is Gibbs free energy,  $K_i$  is the inhibition constant of the reaction,  $T$  is the temperature (298.15 K), and  $R$  stands for the gas constant (1,987. K<sup>-1</sup>. mol<sup>-1</sup>).

Based on table 4, the inhibition constant of the top ten lowest docking scores of propolis compounds was observed. This coefficient is also defined as the concentration required to produce half of the maximum inhibition. According to table 4,  $K_i$  was minimal with an increasing negative docking score. The lower value of  $K_i$  indicated a more potent inhibition activity, with less concentration required to inhibit PAK1.

### Interaction profile

Based on fig. 2, the 2D interactions between PAK1 and its original ligand (G-5555) show the interaction between PAK1 and the five lowest docking score compounds. In addition, fig. 3 indicates the 3D interaction of PAK1 towards G-555, Glyurallin B, and Glyasperin A within the same binding pocket.

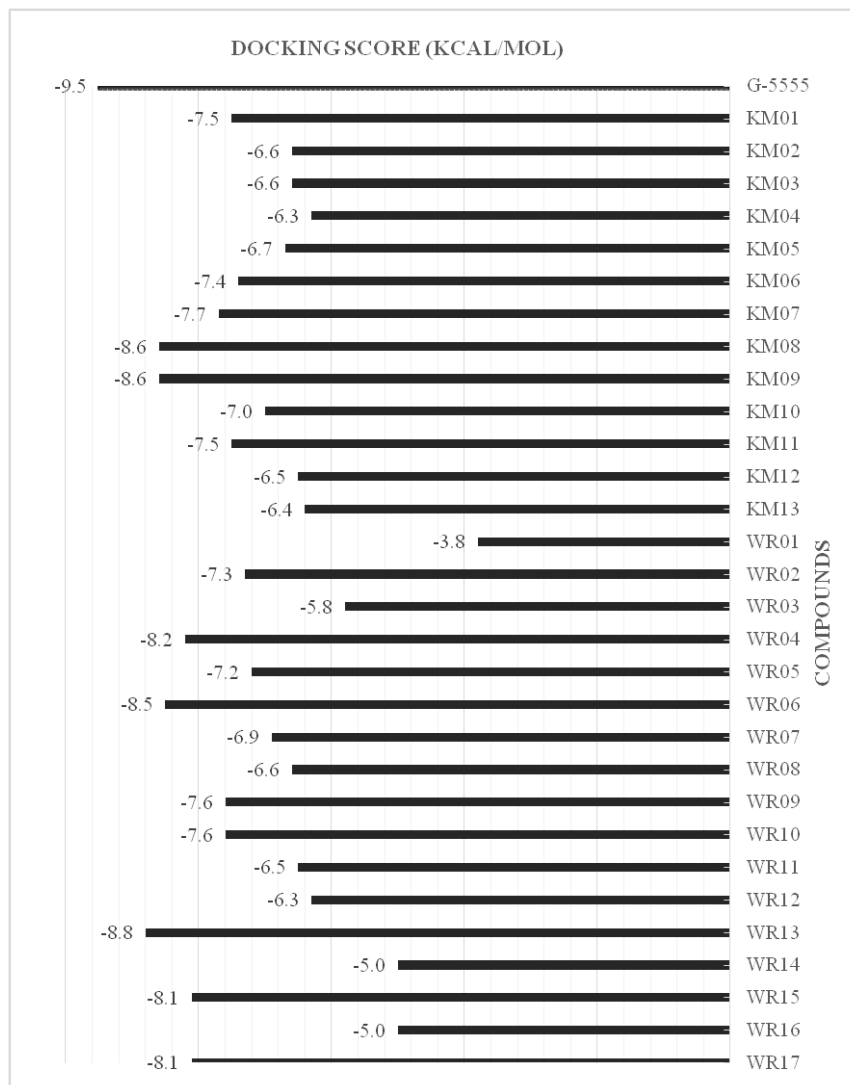


Fig. 1: The docking score between the 30 propolis compounds of *Tetragonula sp.* towards PAK1

Table 4: The top ten propolis compounds with the lowest docking score towards PAK1

No	Compounds	Code	$\Delta G$ (kcal/mol)	$K_i^1$ ( $\mu M$ )
	Positive Control: G-5555	-	-9.5	0.108577
1	Glyurallin B	WR13	-8.8	0.353909
2	Glyasperin A	KM08	-8.6	0.49603
3	Brousoflavonol F	KM09	-8.6	0.49603
4	1,5-Dimethyl-4-[[[2-methyl-6-phenylthieno[2,3-d]pyrimidin-4-yl]hydrazinylidene]methyl]pyrrole-2-carbonitrile	WR06	-8.5	0.587241
5	Yucalexin B7	WR04	-8.2	0.974407
6	Macarangin	WR15	-8.1	1.153582
7	Oleandrigenin	WR17	-8.1	1.153582
8	Isocalopolyanic acid	KM07	-7.7	2.266108
9	Dulxanthone C	WR09	-7.6	2.682802
10	Sulabiroidin A	KM01	-7.5	3.176119

<sup>1</sup> $K_i$ =Inhibition constant

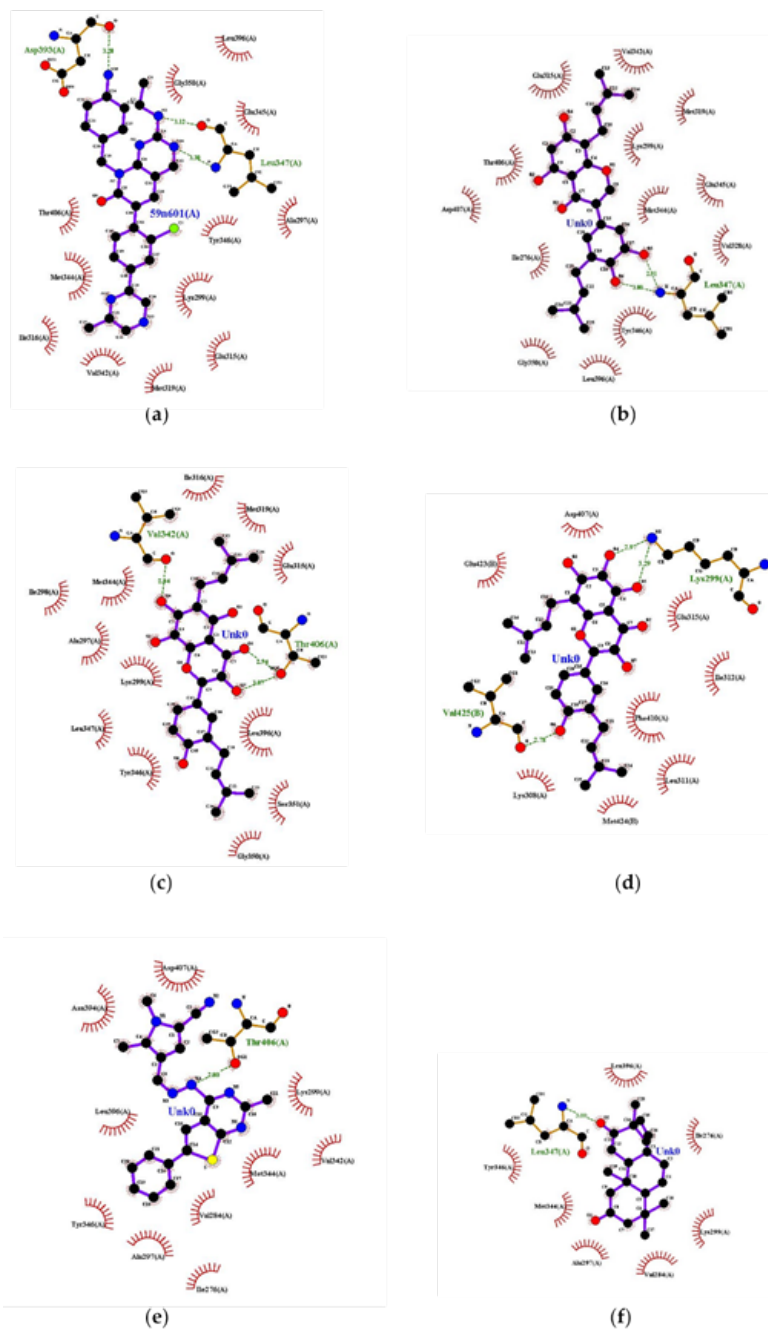


Fig. 2: 2D interaction profiles between PAK1 towards a) G-5555; b) Glyurallin B; c) Glyasperin A; d) Brousoflavonol F; e) 1,5-Dimethyl-4-[[[2-methyl-6-phenylthieno[2,3-d]pyrimidin-4-yl]hydrazinylidene]methyl]pyrrole-2-carbonitrile; f) Yucalexin B7

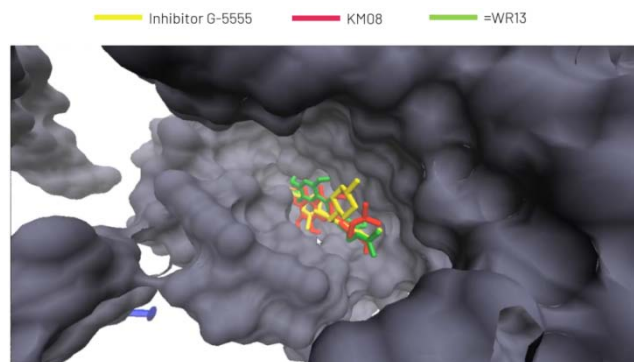


Fig. 3: 3D interaction profiles between PAK1 towards G-5555, Glyurallin B, and Glyasperin A

The visual profiling of 2D bonds was performed using Ligplot+(European Bioinformatics Institute, United Kingdom). This was used to analyze the interactions within the docking area below 5 Å, based on hydrogen bonds and hydrophobic reactions [21, 22]. In the ligand, the bonds and proteins were observed to be purple and brown colorations, respectively. Furthermore, the green dotted line connecting the ligand to the receptor represented a hydrogen bond,

with the numbers observed indicating its length. In addition, the hydrophobic interaction was denoted by a brown fan-shaped structure. Meanwhile, the ligand atoms were shown by reddish-brown "glow" lines. Therefore, the blue, black, yellow, red, and purple colors represented nitrogen, carbon, sulfur, oxygen, and phosphorus. The list of the PAK1 amino acid residues interacting with the five propolis compounds having the lowest docking score is presented in table 5.

**Table 5: The list of the PAK1 amino acid residues interacting with five propolis compounds having the lowest docking score**

Compound	Hydrogen bonds	Hydrophobic interactions
Glyurallin B	Leu 347, Leu347	Val342, Met319, Lys299, Glu345, Met344, Val328, Tyr346, Leu396, Gly350, Ile276, Asp407, Thr406, Glu315
Glyasperin A	Val342, Thr406	Ile316, Met319, Glu315, Leu396, Ser351, Gly350, Tyr346, Leu347, Lys299, Ala297, Ile298, Met344, Val342, Ile316, Met344, Thr406
Brousoflavonol F	Lys299, Lys299, Val425	Asp407, Glu423, Lys308, Met424, Leu311, Phe410, Ile312, Glu315
1,5-Dimethyl-4-[[[2-methyl-6-henylthieno[2,3-d]pyrimidin-4-yl) hydrazinylidene] methyl] pyrrole-2-carbonitrile	Thr406	Val342, Ile316, Met344, Thr406, Asp407, Asn394, Leu396, Tyr346, Ala297, Ile276, Val284, Met344, Val342, Lys299
Yucalexin B7	Leu347	Val342, Ile316, Met344, Thr406, Leu396, Ile276, Lys299, Val284, Ala297, Met344, Tyr346

To understand the interaction profile, the key residues of PAK1 should be acknowledged. These include Glu345 and Leu347, which are residues in the active site of PAK1 [23, 24] and are essential for the binding of ATP-competitive inhibitors. Most of the existing synthetic PAK1 residues functioned as ATP-competitive inhibitors [24]. Based on this study, Glyurallin B had hydrophobic interaction with these residues. The following essential residue is the Glu315, which is responsible for the selective binding of PAK1 inhibitors [24]. This indicated that the presence of the residue had advantages on the active sites of PAK1, compared to the Glu345 and Leu347. Based on this study, Glyasperin A and Brousoflavonol F had interactions with the Glu315 through hydrophobic reaction.

Another essential residue is the Met344, which acts as a gatekeeper in PAK protein [24]. This residue is known to partially or wholly block the hydrophobic region present in the ATP binding pocket. The presence of Met344 also contributes to the selectivity of the kinase against the entry of small molecular inhibitors. This indicates that the smaller size of the residue leads to easier inhibitor entry through the "gate" of the binding pocket hydrophobic region. In this study, all five compounds, except Brousoflavonol F, had interactions with Met344. The following vital residues are the Thr406 and Asp406, which act as DFG motif compounds on PAK1 protein [24]. The results showed that all five compounds had interactions with these residues. According to Schroder *et al.*, the DFG motif residue controlled the binding mode and affinity of the inhibitor [25]. This indicated that targeting the Thr406 and Asp406 increased the activity and selectivity profile of the chosen inhibitor, leading to an attractive strategy to be developed in the search for selective protein kinase remnants. Based on the knowledge of the molecular docking simulations in this study, the potential for *Tetragonula* sp. propolis compounds to be PAK1 inhibitors was observed.

#### Synergistic effect

The next question is based on understanding whether the information obtained was effective in developing COVID-19 therapeutics through the following comparisons, (1) using enough five compounds with the most potential, and (2) using the entire propolis. Based on this condition, a literature study was conducted to determine the methods by which these comparisons were observed to have specific biological activities. This was due to understanding whether there was a synergistic effect on the propolis compounds. Synergy is defined as the combinative effects of more significant compounds. This indicated more effectiveness in using a combination of compounds to achieve desired goals.

Several previous studies showed a synergistic effect on propolis, such as Oses *et al.* [26]. It evaluated antioxidant activity impacts through five main flavonoid propolis compounds, compared to the

utilization of the whole element [26]. The results showed that propolis highly suppressed the formation of oxidants than the use of individual or combination of 5 flavonoid compounds. This indicated a synergistic effect on propolis. Moreover, several studies focused on the synergism of many propolis compounds compared to individual utilization. For example, Kharsany *et al.* [27] showed that the use of 3 flavonoid propolis compounds had higher anti-microbial activity than individual utilization. Besides this, some studies focused on evaluating the synergism of propolis when combined with other ingredients. For example, Al-Waili *et al.* [28] focused on the synergistic effect of propolis-honey on anti-microbial activity (*C. Albicans*, *S. aureus*, and *E. coli*). This showed that the combination of propolis-honey had higher anti-microbial activity than those individually utilized. Drigla *et al.* [29] also showed the synergistic effect of propolis with other ingredients, where compound combinations and bee venom had higher anti-proliferative activity in breast cancer cells. This indicated that there was a synergistic effect among the compounds present in propolis. Although the analysis carried out in points 4.3 and 4.4 showed the five highest compounds with COVID-19 therapeutic potentials, the application of the entire propolis was still used as a medicinal agent. To validate this result, further studies were needed to determine whether the synergistic effect of the propolis compounds was required for COVID-19 therapeutics.

#### CONCLUSION

Based on the docking score, inhibition constant, and interaction profiles, the best top five propolis compounds obtained PAK1 inhibitor potentials. Meanwhile, propolis compounds demonstrated synergistic effects according to several previous studies. This indicated that propolis was collectively better when used to generate extensive biological activities compared to being utilized as an individual compound. Therefore, *Tetragonula* sp. was promoted as the alternative for COVID-19 treatment due to being a PAK-1 inhibitor.

#### ACKNOWLEDGMENT

The authors would like to thank The Ministry of Education, Culture, Research, and Technology Republic of Indonesia for financial support through PDUPT Grant (No NKB-206/UN2. RST/HKP. OS. OA/2021).

#### FUNDING

Grant Penelitian Dasar Unggulan Perguruan Tinggi (PDUPT) Grant No NKB-206/UN2. RST/HKP. OS. OA/2021.

#### AUTHORS CONTRIBUTIONS

All authors equally contributed to this study.

## CONFLICT OF INTERESTS

No conflicting interests.

## REFERENCES

- World Health Organization. Coronavirus disease 2019 (COVID-19) Situation Report. Available from: <https://www.who.int>. [Last accessed on 01 Dec 2021]
- Kumar D, Chauhan G, Kalra S, Kumar B, Gill MS. A perspective on potential target proteins of COVID-19: comparison with SARS-CoV for designing new small molecules. *Bioorg Chem.* 2020;104:104326. doi: 10.1016/j.bioorg.2020.104326, PMID 33142431.
- Lengauer T, Rarey M. Computational methods for biomolecular docking. *Curr Opin Struct Biol.* 1996;6(3):402-6. doi: 10.1016/s0959-440x(96)80061-3, PMID 8804827.
- Chaudhary K, Mishra N. A review on molecular docking: a novel tool for drug discovery. *JSM Chem.* 2016;4(2):1029.
- Pinzi L, Rastelli G. Molecular docking: shifting paradigms in drug discovery. *Int J Mol Sci.* 2019;20(18):4331. doi: 10.3390/ijms20184331, PMID 31487867.
- Lu S, Strand KA, Mutryn MF, Tucker RM, Jolly AJ, Furgeson SB. PTEN (phosphatase and tensin homolog) protects against Ang II (angiotensin II)-induced pathological vascular fibrosis and remodeling-brief report. *Arterioscler Thromb Vasc Biol.* 2020;40(2):394-403. doi: 10.1161/ATVBAHA.119.313757, PMID 31852223.
- Chen IY, Chang SC, Wu HY, Yu TC, Wei WC, Lin S. Upregulation of the chemokine (C-C motif) ligand 2 via a severe acute respiratory syndrome coronavirus spike-ACE2 signaling pathway. *J Virol.* 2010;84(15):7703-12. doi: 10.1128/JVI.02560-09, PMID 20484496.
- Chu CK, Gadthula S, Chen X, Choo H, Olgen S, Barnard DL. Antiviral activity of nucleoside analogues against SARS-coronavirus (SARS-CoV). *Antivir Chem Chemother.* 2006;17(5):285-9. doi: 10.1177/095632020601700506, PMID 17176633.
- Scorza CA. Propolis and coronavirus disease. 2019 (COVID-19): Lessons from nature. *Complement Ther Clin Pract* 2020;41:101227.
- Berretta AA, Silveira MAD, Condor Capcha JM, De Jong D. Propolis and its potential against SARS-CoV-2 infection mechanisms and COVID-19 disease: running title: propolis against SARS-CoV-2 infection and COVID-19. *Biomed Pharmacother.* 2020;131:110622. doi: 10.1016/j.biopha.2020.110622, PMID 32890967.
- Dimitri B, Katerina D, Viktor S, Maja D. Back to the basics: propolis and COVID-19. *Dermatol Ther.* 2020;33:4.
- Sahlan M, Irdiani R, Flamandita D, Aditama R, Alfarraj S, Ansari MJ. Molecular interaction analysis of sulawesi propolis compounds with SARS-CoV-2 main protease as a preliminary study for COVID-19 drug discovery. *J King Saud Univ Sci.* 2021;33(1):101234. doi: 10.1016/j.jksus.2020.101234. PMID 33223766.
- Miyata R, Sahlan M, Ishikawa Y, Hashimoto H, Honda S, Kumazawa S. Propolis components from stingless bees collected on south Sulawesi, Indonesia, and their xanthine oxidase inhibitory activity. *J Nat Prod.* 2019;82(2):205-10. doi: 10.1021/acs.jnatprod.8b00541, PMID 30719922.
- Cole JC, Murray CW, Nissink JW, Taylor RD, Taylor R. Comparing protein-ligand docking programs is difficult. *Proteins.* 2005;60(3):325-32. doi: 10.1002/prot.20497, PMID 15937897.
- Lipinski CA, Lombardo F, Dominy BW, Feeney PJ. Experimental and computational approaches to estimate solubility and permeability in drug discovery and development settings. *Adv Drug Deliv Rev.* 2001;46(1-3):3-26. doi: 10.1016/s0169-409x(00)00129-0. PMID 11259830.
- Veber DF, Johnson SR, Cheng HY, Smith BR, Ward KW, Kopple KD. Molecular properties that influence the oral bioavailability of drug candidates. *J Med Chem.* 2002;45(12):2615-23. doi: 10.1021/jm020017n, PMID 12036371.
- Quimque MTJ, Notarte KIR, Fernandez RAT, Mendoza MAO, Liman RAD, Lim JAK. Virtual screening-driven drug discovery of SARS-CoV2 enzyme inhibitors targeting viral attachment, replication, post-translational modification and host immunity evasion infection mechanisms. *J Biomol Struct Dyn.* 2021;39(12):4316-33. doi: 10.1080/07391102.2020.1776639.
- Swiss ADME. A free web tool to evaluate pharmacokinetics, drug-likeness and medicinal chemistry friendliness of small molecules. *Sci Rep.* 2017;7:42717.
- Trott O, Olson AJ. AutoDock Vina: improving the speed and accuracy of docking with a new scoring function, efficient optimization, and multithreading. *J Comput Chem.* 2010;31(2):455-61. doi: 10.1002/jcc.21334, PMID 19499576.
- Sharifi M, Raevsky AV, Ghafourian T. Effect of molecular structure, substrate and docking scores on the prediction of the inhibition constants of P-glycoprotein inhibitors. *J Drug Metab Toxicol.* 2016;07(4):2. doi: 10.4172/2157-7609.1000217.
- Wallace AC, Laskowski RA, Ligplot TJM. A program to generate schematic diagrams of protein-ligand interactions. *Protein Eng Design.* 1995;8:127-34.
- Dannenbergh JJ. An introduction to hydrogen bonding by George A. Jeffrey (University of Pittsburgh). Oxford University Press: New York and Oxford. *J Am Chem Soc.* 1998;120(22):5604. doi: 10.1021/ja9756331.
- Shahinozzaman M, Ishii T, Takano R, Halim MA, Hossain MA, Tawata S. Cytotoxic desulfated saponin from *Holothuria atra* predicted to have high binding affinity to the oncogenic kinase PAK1: A combined *in vitro* and *in silico* study. *Sci Pharm.* 2018;86(3):32. doi: 10.3390/scipharm86030032, PMID 30200330.
- Shahinozzaman M, Ishii T, Ahmed S, Halim MA, Tawata S. A computational approach to explore and identify potential herbal inhibitors for the p21-activated kinase 1 (PAK1). *J Biomol Struct Dyn.* 2020;38(12):3514-26. doi: 10.1080/07391102.2019.1659855, PMID 31448698.
- Schroder M, Bullock AN, Fedorov O, Bracher F, Chaikuad A, Knapp S. DFG-1 residue controls inhibitor binding mode and affinity, providing a basis for the rational design of kinase inhibitor selectivity. *J Med Chem.* 2020;63(18):10224-34. doi: 10.1021/acs.jmedchem.0c00898, PMID 32787076.
- Oses SM, Marcos P, Azofra P, de Pablo A, Fernandez Muino MA, Sancho MT. Phenolic profile, antioxidant capacities and enzymatic inhibitory activities of propolis from different geographical areas: needs for analytical harmonization. *Antioxidants (Basel).* 2020;9(1):75. doi: 10.3390/antiox9010075, PMID 31952253.
- Kharsany K, Viljoen A, Leonard C, van Vuuren SV. The new buzz: investigating the antimicrobial interactions between bioactive compounds found in South African propolis. *J Ethnopharmacol.* 2019;238:111867. doi: 10.1016/j.jep.2019.111867, PMID 30978456.
- Al-Waili N, Al-Ghamdi A, Ansari MJ, Al-Attal Y, Salom K. Synergistic effects of honey and propolis toward drug multi-resistant staphylococcus aureus, Escherichia coli and Candida albicans isolates in single and polymicrobial cultures. *Int J Med Sci.* 2012;9(9):793-800. doi: 10.7150/ijms.4722, PMID 23136543.
- Drigla F, Balacescu O, Visan S, Bisboaca SE, Berindan Neagoe I, Marghitas LA. Synergistic effects induced by combined treatments of aqueous extract of propolis and venom. *Clujul Med.* 2016;89(1):104-9. doi: 10.15386/cjmed-527, PMID 27004032.